PROCEEDINGS OF SCIENCE

D meson production cross sections at ATLAS

Simon Head[*†]
University of Birmingham
E-mail: simon.head@cern.ch

The production of $D^{*\pm}$, $D^{\pm}$ and $D_s^{\pm}$ charmed mesons has been measured with the ATLAS detector in pp collisions at $\sqrt{s} = 7$ TeV using an integrated luminosity of 1.1 nb^{-1}. The charmed mesons have been reconstructed in the range of transverse momentum $p_{\mathrm{T}}(D^{(*)}) > 3.5$ GeV and pseudorapidity $|\eta(D^{(*)})| < 2.1$. In addition to integrated cross sections in this visible region, differential cross sections as a function of transverse momentum and pseudorapidity were measured for $D^{*\pm}$ and $D^{\pm}$ production. The NLO QCD predictions are consistent with the data in the visible kinematic region within the large theoretical uncertainties.

ATL-PHYS-PROC-2011-034
20 May 2011

The 13th International Conference on B-Physics at Hadron Machines
April 4-8 2011
Amsterdam, The Netherlands

[*]Speaker.
[†]On behalf of the ATLAS collaboration.

1. Introduction

A study of $D^{*\pm}$, $D^{\pm}$ and $D_s^{\pm}$ reconstruction with the ATLAS detector [1] was presented in [2]. The analysis presented here details a measurement of the production cross sections of the charmed mesons along with a comparison to next-to-leading order (NLO) QCD calculations [3].

The $D^{*\pm}$, $D^{\pm}$ and $D_s^{\pm}$ charmed mesons were reconstructed in the range of transverse momentum $p_{\mathrm{T}}(D^{(*)}) > 3.5$ GeV and pseudorapidity $|\eta(D^{(*)})| < 2.1$ using tracks measured in the ATLAS Inner Detector. Contributions from both charm hadronisation and beauty hadronic decays are included in the measured visible $D^{(*)}$ production cross sections and NLO QCD predictions. The Monte Carlo predicts a contribution of about 10% from beauty hadron decays to the reconstructed signals.

The data sample used in this analysis was collected between March and July 2010. To trigger events the Minimum Bias Trigger Scintillator (MBTS) and random triggers were used, which are unbiased for events of interest [4]. However, the triggers were prescaled after the initial data taking period. Taking into account the trigger prescale and random factors, the data sample corresponds to an integrated luminosity of 1.07 ± 0.12 nb^{-1}.

The $D^{*\pm}$ mesons were identified using the decay channel $D^{*+} \to D^0\pi_s^+ \to (K^-\pi^+)\pi_s^+$, where the pion from the D^{*+} decay is referred to as the 'soft' pion, π_s. The transverse decay length of the D^0 candidates was required to satisfy $L_{XY} > 0$. The left plot in Figure 1 shows the distribution of the mass difference, $\Delta M = M(K\pi\pi_s) - M(K\pi)$, for $D^{*\pm}$ candidates. A mass window is made on $M(K\pi)$. To take the mass resolution into account the consistency requirement was $1.80 < M(K\pi) < 1.93$ GeV for $p_{\mathrm{T}}(D^{*\pm}) > 12$ GeV or $|\eta(D^{*\pm})| > 1.3$, and $1.82 < M(K\pi) < 1.91$ GeV otherwise. A clear signal is seen at the nominal value of $M(D^{*\pm}) - M(D^0)$. The right plot in Figure 1 shows the $M(K\pi)$ distribution for the $D^{*\pm}$ candidates which satisfy $144 < \Delta M < 147$ MeV. A clear signal is seen, consistent with the PDG world average value of $M(D^0)$ [5]. The dashed histograms show the distributions for wrong charge combinations, in which both tracks forming the D^0 candidate have the same charge and the third track has the opposite charge.

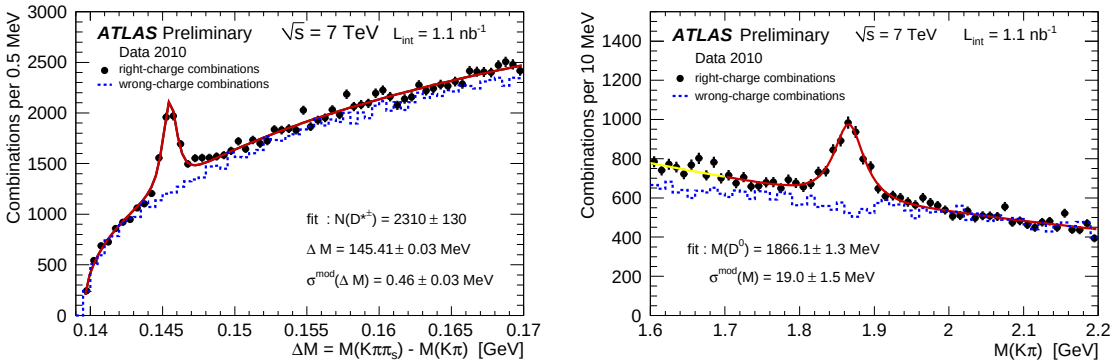

Figure 1: The distribution of the mass difference $\Delta M = M(K\pi\pi_s) - M(K\pi)$ (left plot) and the $M(K\pi)$ distribution (right plot) for the $D^{*\pm}$ candidates (points). The dashed histograms show the distributions for wrong charge combinations and the solid curves represent the fit results. The $M(K\pi)$ range below 1.7 GeV was excluded from the fit because of contributions from other D^0 decay modes.

The $D^{\pm}$ mesons were reconstructed from the decay $D^+ \to K^-\pi^+\pi^+$. The transverse decay length of the $D^{\pm}$ candidates was required to be at least 1.2 mm. Figure 2 shows the $M(K\pi\pi)$ distribution of the $D^{\pm}$ candidates after all cuts. A clear signal is seen that is consistent with the PDG world average D^+ mass.

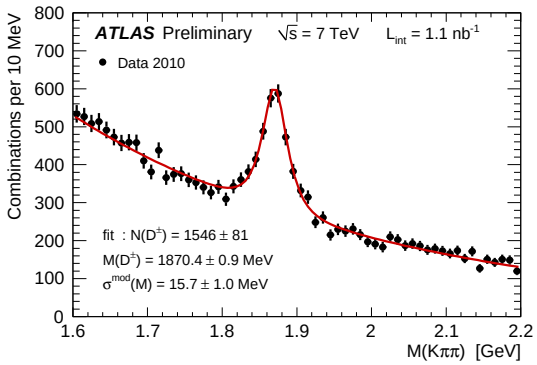

Figure 2: The $M(K\pi\pi)$ mass distribution for the $D^{\pm}$ candidates (points). The solid curve represents the fit results.

The $D_s^{\pm}$ mesons were reconstructed from the decay $D_s^+ \to \phi\pi^+$ with $\phi \to K^+K^-$. The transverse decay length of the $D_s^{\pm}$ candidate was required to satisfy $L_{XY}(D_s^{\pm}) > 0.4$ mm. The left plot in Figure 3 shows the $M(KK\pi)$ distribution for the $D_s^{\pm}$ candidates with $M(KK)$ within 6 MeV of the PDG ϕ mass. A clear signal is consistent with the PDG world average value of $M(D_s^+)$. A second marginal signal is visible around $M(D^+)$, expected from the decay $D^+ \to \phi\pi^+$ with $\phi \to K^+K^-$. Monte Carlo studies estimated that the $M(KK\pi)$ distribution contained no sizeable contamination originating from $D^+ \to K^-\pi^+\pi^+$ decays. The right plot in Figure 3 shows the $M(KK)$ distribution for $D_s^{\pm}$ candidates that satisfy $1.93 < M(KK\pi) < 2.01$ GeV. A clear signal is seen that is consistent with the PDG world average value of $M(\phi)$.

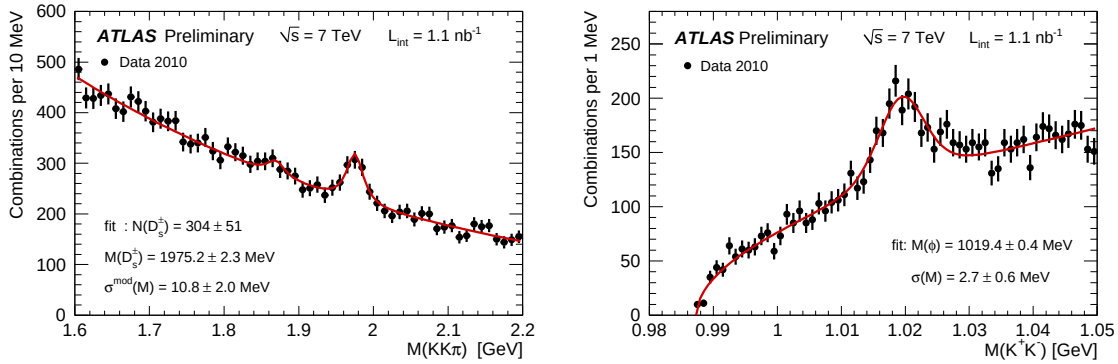

Figure 3: $M(KK\pi)$ mass distribution for the $D_s^{\pm}$ candidates (left plot) and $M(KK)$ distribution (right plot). The solid curves represent the fit results.

The fitted masses of the reconstructed charmed mesons were found to be in agreement with their world averages [5] and the observed mass resolutions agree with Monte Carlo expectations.

2. Cross sections

The visible $D^{(*)}$ production cross sections were measured for the process $pp \to D^{(*)}X$ in the kinematic region $p_{\mathrm{T}}(D^{(*)}) > 3.5$ GeV and $|\eta(D^{(*)})| < 2.1$. The cross section for a given charmed meson was calculated using

$$\sigma_{pp\to D^{(*)}X} = \frac{N(D^{(*)})}{\mathscr{A}\cdot\mathscr{L}\cdot\mathscr{B}}, \tag{2.1}$$

where $N(D^{(*)})$ is the number of reconstructed charmed mesons in data, $\mathscr{A}$ is the reconstruction acceptance obtained from the Monte Carlo, $\mathscr{L}$ is the integrated luminosity of the data sample and $\mathscr{B}$ is the branching fraction or the product of the branching fractions for the relevant decay channel [5]. The acceptance takes into account efficiencies, migrations and small contributions of other decay modes. The visible cross sections for $D^{(*)}$ mesons in this kinematic range are measured to be

$$\begin{aligned}
\sigma^{vis}(D^{*\pm}) &= 285 \pm 16(\text{stat.})\,{}^{+32}_{-27}(\text{syst.}) \pm 31(\text{lumi.}) \pm 4(\text{br.})\ \mu\text{b},\\
\sigma^{vis}(D^{\pm}) &= 238 \pm 13(\text{stat.})\,{}^{+35}_{-23}(\text{syst.}) \pm 26(\text{lumi.}) \pm 10(\text{br.})\ \mu\text{b},\\
\sigma^{vis}(D_s^{\pm}) &= 168 \pm 34(\text{stat.})\,{}^{+27}_{-25}(\text{syst.}) \pm 18(\text{lumi.}) \pm 10(\text{br.})\ \mu\text{b},
\end{aligned} \tag{2.2}$$

where the last two uncertainties are due to the luminosity measurement and the charmed meson decay branching fractions. The NLO POWHEG-PYTHIA predictions are

$$\begin{aligned}
\sigma^{vis}(D^{*\pm}) &= 153\,{}^{+169}_{-80}(\text{scale})\,{}^{+13}_{-15}(m_Q)\,{}^{+24}_{-21}(\text{PDF})\,{}^{+20}_{-16}(\text{hadr.})\ \mu\text{b},\\
\sigma^{vis}(D^{\pm}) &= 132\,{}^{+137}_{-65}(\text{scale})\,{}^{+11}_{-10}(m_Q)\,{}^{+20}_{-18}(\text{PDF})\,{}^{+21}_{-11}(\text{hadr.})\ \mu\text{b},\\
\sigma^{vis}(D_s^{\pm}) &= 59\,{}^{+57}_{-28}(\text{scale})\,{}^{+4}_{-6}(m_Q)\,{}^{+9}_{-8}(\text{PDF})\,{}^{+7}_{-8}(\text{hadr.})\ \mu\text{b}.
\end{aligned} \tag{2.3}$$

The differential cross sections $d\sigma/dp_{\mathrm{T}}$ and $d\sigma/d|\eta|$ for $D^{*\pm}$ and $D^{\pm}$ production are compared in Figures 4 and 5 with the NLO QCD predictions. A differential cross section measurement has not yet been performed for $D_s^{\pm}$ due to the limited statistics in the current data sample. The data points are drawn at the bin centres of gravity in the $d\sigma/dp_{\mathrm{T}}$ distributions and at the bin centres in the $d\sigma/d|\eta|$ distributions. The bin centre of gravity is defined as the point at which the value of the exponential function, describing the distribution slope, equals the mean value of the function in the bin. The NLO QCD predictions are consistent with the data in the measured $p_{\mathrm{T}}(D^{(*)})$ and $|\eta(D^{(*)})|$ ranges within the large theoretical uncertainties.

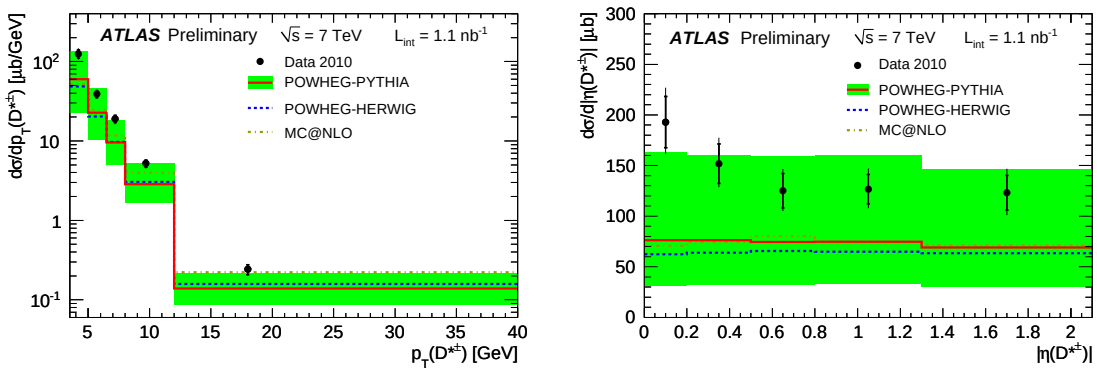

Figure 4: Differential cross sections for $D^{*\pm}$ mesons as a function of p_{T} (left) and $|\eta|$ (right) for data (points) compared to the NLO QCD calculations of POWHEG-PYTHIA, POWHEG-HERWIG and MC@NLO (histograms). The data points are drawn at the bin centres of gravity in the $d\sigma/dp_{\mathrm{T}}$ distribution (see text) and at the bin centres in the $d\sigma/d|\eta|$ distribution. The inner error bars show the statistical uncertainties and the outer error bars show the statistical and systematic uncertainties added in quadrature. The bands show the estimated theoretical uncertainty of the POWHEG-PYTHIA calculation.

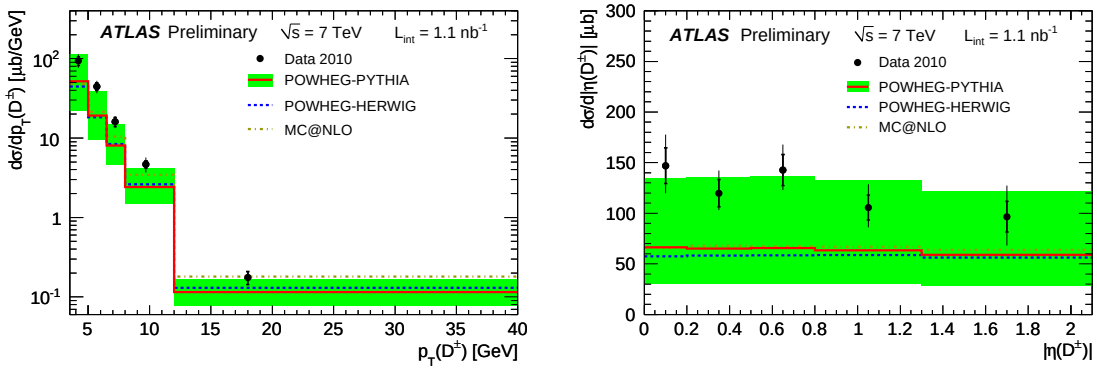

Figure 5: Differential cross sections for $D^{\pm}$ mesons as a function of p_{T} (left) and $|\eta|$ (right) for data (points) compared to the NLO QCD calculations of POWHEG-PYTHIA, POWHEG-HERWIG and MC@NLO (histograms). The data points are drawn at the bin centres of gravity in the $d\sigma/dp_{\mathrm{T}}$ distribution (see text) and at the bin centres in the $d\sigma/d|\eta|$ distribution. The inner error bars show the statistical uncertainties and the outer error bars show the statistical and systematic uncertainties added in quadrature. The bands show the estimated theoretical uncertainty of the POWHEG-PYTHIA calculation.

References

[1] ATLAS Collaboration, *The ATLAS Experiment at the CERN Large Hadron Collider*, *JINST* **3** (2008) S08003.

[2] ATLAS Collaboration, *$D^{(*)}$ mesons reconstruction in pp collisions at $\sqrt{s} = 7$ TeV*, ATLAS-CONF-2010-034.

[3] ATLAS Collaboration, *Measurement of $D^{(*)}$ meson production cross sections in pp collisions at $\sqrt{s} = 7$ TeV*, ATLAS-CONF-2011-017.

[4] ATLAS Collaboration, *Performance of the Minimum Bias Trigger in $p-p$ Collisions at $\sqrt{s} = 7$ TeV*, ATLAS-CONF-2010-068.

[5] K. Nakamura et al. (Particle Data Group), *The Review of Particle Physics*, *J. Phys.* **G37** (2010) 075021.